IJCRT.ORG ISSN : 2320-2882

INTERNATIONAL JOURNAL OF CREATIVE RESEARCH THOUGHTS (IJCRT)

An International Open Access, Peer-reviewed, Refereed Journal

ECO – FRIENDLY SYNTHESIZED CR_2O_3/SIO_2/GO CORE SHELL NANOPARTICLES BY *ARISTOLOCHIA INDICA* AND THEIR OPTO – STRUCTURAL ANALYSIS – OVERVIEW

S. Thangeswari[1], S. Arul vathana[2], Dr. K. Amudhavalli[3], C. Infant Francita Fonseka[4], T. Vinoline Golda[5]

[1] Research Scholar, Registration No.19132232132026, [2] Research Scholar, Registration No.19212232132025, [3]Associate Professor, [4]Research Scholar, Registration No. 20212232132010, [5]Research Scholar, Registration No.20112232132012

[12345]Department of Physics, V.O.Chidambaram College, Thoothukudi- 628 008, Tamil Nadu, India.

[12345]*Affiliated to Manonmaniam Sundaranar University, Abishekapatti, Tirunelveli- 627 012, Tamil Nadu, India.*

***Abstract*:**In this work, Graphene based Silica coated Chromium oxide nanoparticles were synthesized by biological method using *Aristolochia Indica* extract in which enzymes converted metal salts into nanoparticles. These particles were characterized by XRD (X-ray Diffraction), EDX (Energy Dispersive X-Ray Spectroscopy), UV-Vis (Ultraviolet Visible), SEM (Scanning Electron Microscopy) and Electrochemical Analysis. The size of nanoparticles of Cr_2O_3 core, Cr_2O_3 /SiO_2 core shell and Cr_2O_3/SiO_2 /GO were 58, 40 and 17 nm respectively. SEM showed well-defined and rods with width 27, 21 and 10 nm range. The Cr_2O_3/SiO_2/GO core shell nanoparticles were studied towards optical, optoelectronic and specific capacitance for energy devices.

***Keywords*: Aristolochia Indica, Green synthesis, core shell, optical analysis, Electrochemical Analysis.**

1. INTRODUCTION

Among other metal oxides, Cr_2O_3 is more observable because of their specific thermodynamic stability, hardness, chemical resistance and anti-ferromagnetic properties. Also, Cr_2O_3 is behaving n-type and p-type semiconductor. Previously, several groups have researched applications based on Cr_2O_3 NPs and a variety of applications, such as sensors, green pigment and protective coating, solar cell, fuel cell, piezoelectric devices, have been achieved (Choi.S et al., 2018). Moreover, Cr_2O_3 NPs plays a great role in the domain of pharmacy and medicine such as antibacterial, anticancer, antileshmanial, enzyme inhibition and antioxidant agents due to their reliable curative biomedical applications.

The multifunctional applications and appealing properties of Cr_2O_3 NPs have led to a captivating interest in their synthesis of a commercially viable and greener process. Many physical and chemical procedures have been proposed for the fabrication of Cr_2O_3 NPs such as thermal decomposition (Guo, Yu et al., 2019), sol-gel (Rasheed et al., 2020), solvothermal, chemical precipitation, electrochemical method, precipitation method, mechanical grinding, arc discharge method, co-precipitation and template method. Previously, while being effectual, the physical processes are compromised due to their energy requirements and costly equipment. Therefore, the green chemical reduction methods by including plant extracts as bio-reductants are becoming popular (Ghotekar.S et al., 2021).

The synthesis of core/shell structured material provides the supporting behavior between the core and shell materials. SiO_2 assisted core shell Nano structure materials have great attention to its top grade such as good environmental stability, compatibility with other materials and ease in preparation (Kiumars Bahrami et al., 2018). Silica materials provide excellent physicochemical, mechanical and optical properties and are widely used in high-tech applications. The unique optical properties of SiO_2 nanoparticles observed at the nano-scale have been largely attributed to the defects present at the surface. Silica nanoparticles have been intensively studied to determine their size-dependent physicochemical properties and unique optical properties at smaller size. The increase in optical fluorescence intensity for stilbene 420 in mesoporous silica nanoparticles would make these nanomaterials more useful for nanosensors and nanolasers application (Haque, Fozia Z et al., 2016). Graphene, a prominently one- atom-thick carbon material has become a new favorite to fabricate functional hybridized materials. GO sheet contains a mixture of elec-tronically conducting sp^2 and insulating sp^3carbon atoms. Several studies have used GO in nanocomposite preparation not only for its good NLO properties, but

also due to its ease of preparation, easily dispersed in water, low cost of fabrication,and its thin film can be easily fabricated on different types of substrates (Asmaa M et al., 2021). Owing to its excellent physical and chemical properties, graphene is considered as a potential candidate for large number of applications in many technological fields such as nanoelectronics, composites, energy storage devices, efficient lasers, photodetectors, and biomedical applications (Sumit Ranjan Sahu et al., 2013).

In the present study, Cr_2O_3 core is developed using Aristolochia Indica natural extract through Bio synthesis process. The morphological and optical characterization of core Cr_2O_3, core shell Cr_2O_3/SiO_2 and $Cr_2O_3/SiO_2/GO$ nanoparticles were studied towards optical and optoelectronic devices.

2. DEVELOPMENT OF CR2O3/SIO2/GO CORE SHELL NANOPARTICLES

In this method first of all a Aristolochia Indica stem extract was prepared. Then the salt solution was prepared by dissolving 7 g of salt in 150 ml of deionized water and mixed with 20ml stem extract of aristolochia Indica and stirred for 60 minutes at 35ºC. Then the resultant material was the color of the solution changed from orange to green indicating the formation of chromium oxide core. After that filtered the solid and washed with ethanol. The resultant material was dried at 100ºC in the oven for 3 hours. The brownish colored Cr2O3 cores were obtained through the calcination procedures at the temperatures of 360ºC in a furnace for 6 hours.

5mg o f Cr_2O_3 dissolved in water and ethanol (1:7). The solution was stirred to form a solution. Then the formation of shell by adding 0.5 mL ammonia and 5 drops of TEOS while stirring the Cr_2O_3 suspension with a time interval of 10 s between each TEOS drop. After that, the mixture was stirred continuously for 1 hour. Finally, the suspension was washed with distilled water and Ethanol by centrifugation to separate the core shell particles from the liquid in 50 mL Eppendorf tubes. The final products were dried at 300ºC in the muffle furnace for 1 hour.

For $Cr_2O_3/SiO_2/GO$ nanocomposite, 0.6 mgs of Cr_2O_3/SiO_2 was added to 20 mL of a GO aqueous suspension (1.0 mg/mL) and the resulting solution was aged for 30 min. Again, drop-wise addition of 10 mL of Aristolochia Indica extract into the prepared solution at room temperature with constant stirring for 90 min. Then the resultant solution was decanted and the obtained $Cr_2O_3/SiO_2/GO$ core shell was dried at 100 °C for 24 hours in an oven. Finally black colour $Cr_2O_3/SiO_2/GO$ core shell was collected and used for further studies.

3. RESULT AND DISCUSSION

3.1 X-ray Diffractogram

To highlight the difference between the XRD patterns of core Cr_2O_3, Cr_2O_3/SiO_2 and $Cr_2O_3/SiO_2/GO$ core shell nanoparticles, the XRD pattern of Cr_2O_3 is plotted along with those of pure GO, Cr_2O_3/SiO_2 and Graphene Oxide coated samples in figure 1. The XRD peaks were used to find size of particles and crystallinity. The peaks for Cr_2O_3 core NPs

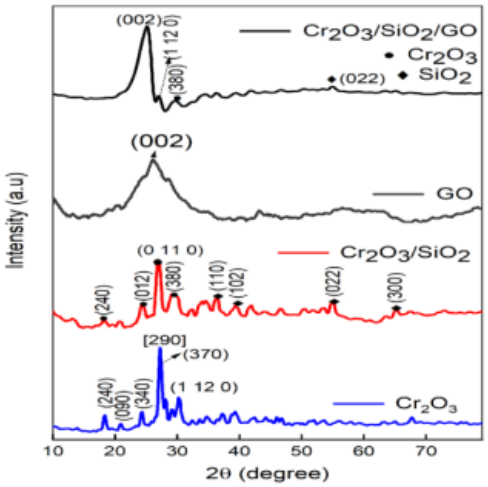

Figure 1. The XRD spectrum of Cr_2O_3 core, Cr_2O_3/SiO_2 core shell and $Cr_2O_3/SiO_2/GO$ NPs

were formed at 2θ values of 18.07°, 21.02°, 24.2°, 26.38°, 27.99° and 30.40° belongs to the hkl plans of (2 4 0), (0 9 0), (3 4 0), (2 9 0), (3 7 0) and (1 12 0) respectively. The peak values are concordant with the JCPDS file no. 361330, which corresponds to orthorhombic structure with the following lattice constant a= 12.01Å, b= 36.60 Å and c= 3.28 Å.

The core Cr_2O_3 nanoparticles were coated with SiO_2 shell, the diffraction patterns were retained with orthorhombic Cr_2O_3 and SiO_2 that shows an orientation along 2θ = 24.19°, 26.94, 29.5, 36.54°, 39.47°, 54.88° and 65.78° belongs to the reflection of (0 1 2), (0 11 0), (3 8 0), (1 1 1), (1 0 2), (0 2 2) and (3 0 0) planes respectively (JCPDS file no. 898934) and were observed that the peaks shifted towards the higher (26.38° - 26.94°). There is no impure phase is observed in the XRD pattern of Cr_2O_3 and Cr_2O_3/SiO_2. It is clearly evident that the formation of phase pure core Cr_2O_3 and core shell Cr_2O_3/SiO_2. Further added in the GO, the XRD pattern of Cr_2O_3/SiO_2 core shell NPs shows phase orthorhombic structured $Cr_2O_3/SiO_2/GO$ core shell NPs planes of (0 0 2), (1 12 0), (3 8 0) and (0 2 2) forming and its corresponding 2θ = 26.5˚, .24.4◦ and 26.8◦ respectively. Since no irrelevant peaks were observed in the diffraction pattern.

It is noticed that when the addition of GO into the core shell Cr_2O_3/SiO_2, the crystallinity of Cr_2O_3/SiO_2 core shell get increased, which will lead to get good power conversion efficiency reported by Daniel T et al ., 2021 and Al-Awadi et al., 2021. By using the scherrer's formula to find crystalline size of core shell NPs (Rasheed et al., 2019). The XRD data shows that the average particle size was 58, 40 and 17 nm for core Cr_2O_3, core shell Cr_2O_3/SiO_2 and Cr_2O_3/SiO_2/GO NPs respectively.

3.2 The morphological analsysis

Fig. 2(a–c) shows the SEM images of core Cr2O3, core shell Cr2O3/SiO2 and Cr2O3/SiO2/GO. The surface of the Cr_2O_3 core shows uniformly distributed grains over the surface which is rod like a shape is shown in Fig. 2 (a). These nanorods were ranged in the length 500 nm, their width is 27 nm, and their thickness is in the range 2–5 nm. After SiO_2 were introduced in the Cr_2O_3 core, the morphology shows (Fig. 2 (b)) irregular particles which are distributed on the entire surface. The typical length of the rods is in the range 100 nm, their width is 21 nm, and their thickness is in the range 1 – 4 nm. While, the GO were added to the core shell

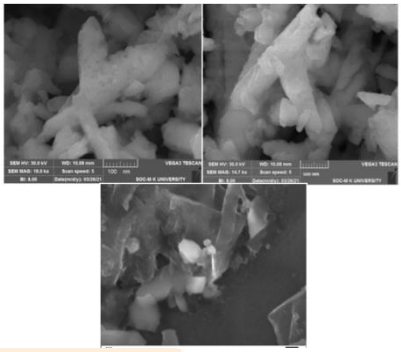

Cr2O3/SiO2, a well defined nanorods are obtained as clearly visualized from Fig. 2 (c).

Figure 2. The SEM Micrographs of core Cr_2O_3,core shell Cr_2O_3/SiO_2 and Cr_2O_3/SiO_2/GO NPs

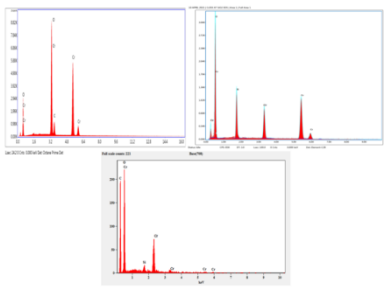

Figure 3. The Energy Dispersive Spectra of the (a) core Cr_2O_3, (b) core shell Cr_2O_3/SiO_2 and (c) Graphene based core shell Cr_2O_3/SiO_2/GO

The nanorods were arranged in the width is 10 nm over the GO sheet, which makes the surface smooth and no cracks are observed. The individual grains were clearly seen and they were fine in nature. The presence of nanorods were important for the development of electronic, optical, magnetic and micromechanical devices reported by Sasani Ghamsari et al., 2019. Fig. 3 shows the energy-dispersive X-ray spectra of core Cr_2O_3/SiO_2/GO core shell. The observed peaks in the EDS data evoked the presence of Cr, O, Si and C signals. From the core Cr_2O_3 and core shell Cr_2O_3/SiO_2 shows the C signals which are arouse during the green process. The EDS table 1 with atomic percentage of elements is given in the supporting information of core Cr_2O_3, core shell Cr_2O_3/SiO_2 and Cr_2O_3/SiO_2/GO nanoparticles.

Table 1. The Energy Dispersive data of the (a) core Cr_2O_3, (b) core shell Cr_2O_3/SiO_2 and (c) $Cr_2O_3/SiO_2/GO$

Cr_2O_3			**Cr_2O_3/SiO_2**			**$Cr_2O_3/SiO_2/GO$**		
Element	Weight%	Atomic%	Element	Weight%	Atomic%	Element	Weight%	Atomic%
O K	23.49	50.29	O K	28.85	52.8	O K	29.02	31.42
C K	8.7	11.16	C K	9.76	10.18	C K	40.61	48.15
Cr K	62.81	38.55	Cr K	46.46	26.95	Cr K	23.23	16.90
			Si K	14.93	10.07	Si K	7.13	3.53
Total		100	Total		100	Total		100

3.3 Functional Group Analysis

Fourier transform infrared spectroscopy (FTIR) Fig. 4 shows the functional group spectra of core Cr_2O_3, core shell Cr_2O_3/SiO_2 and Cr_2O_3/SiO2/GO nanoparticle at room temperatures. FTIR spectroscopy was carried out to ascertain the purity and nature of Chromium or Chromium Oxide nanoparticles. The band between 3300 cm^{-1} to 3400 cm^{-1} are due to the stretching vibration of O–H and 1620 cm^{-1} to 1640 cm^{-1} are due to the C=O stretching and bending vibrations of the sample. The absorption peaks at 2900 cm^{-1} – 2300 cm^{-1} are may be due to C–H stretching vibrations. In addition, the absorption peak at 1459 cm^{-1} – 1479 cm^{-1} was assigned to the bending vibration of the C–H and 1383 cm^{-1} and 1121 m^{-1} could be attributed to the hydroxyl groups associated with the Cr^{3+} ions and the band at 1098 cm^{-1} are assigned to the bending vibration of the Si – O – Si. The peaks at 850 cm^{-1} to 950 cm^{-1} are assigned to Cr – O – Cr vibrations. The peaks at 450 cm^{-1} to 750 cm^{-1} are assigned to O – Cr – O stretching vibrations. The absorption peaks at 619 cm^{-1} from the Cr–O bonds may be covered by the bending vibration of Si – O at 623 cm^{-1}. The absorption peaks of Si–OH at 1098 cm^{-1}. Similar

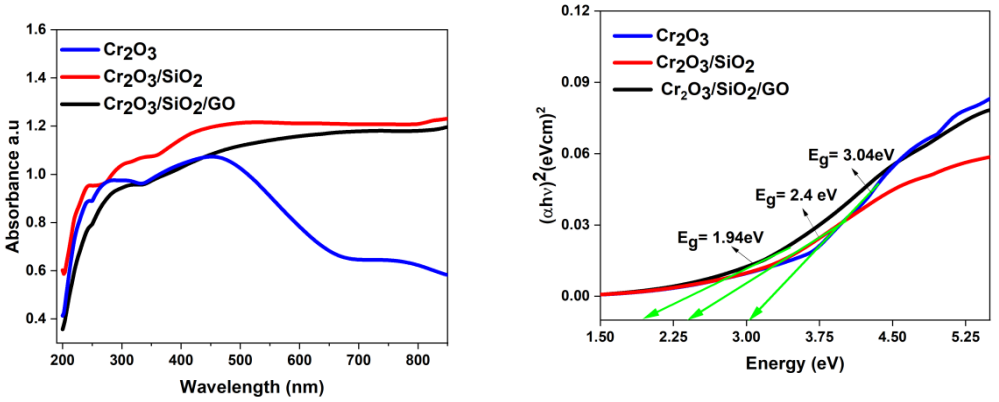

Figure 4 FTIR spectra of core Cr_2O_3, core shell Cr_2O_3/SiO_2 and Graphene coated Cr_2O_3/SiO_2 core shell nanoparticles

3.4 Optical Studies

The UV-Visible analysis was recorded in the range of 200-900 nm. The UV-Visible analysis indicates that Cr_2O_3 core, Cr_2O_3/SiO_2 core shell and $Cr_2O_3/SiO_2/GO$ NPs show maximum absorbance at 200 – 400 nm, which occurs due to resonance of collective conduction electrons with incident electromagnetic radiations respectively Rasheed et al., 2019 and Ghotekar, S et al., 2021.

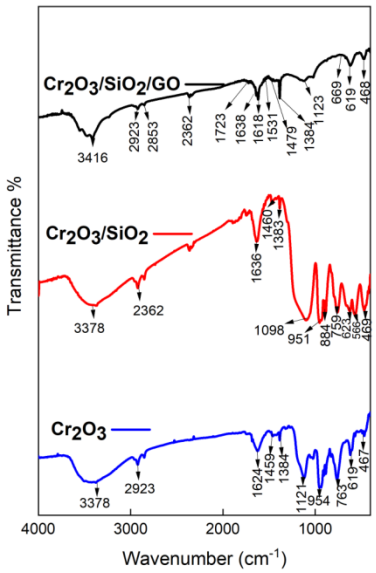

Figure 5 UV and Band gap spectra of core Cr_2O_3, core shell Cr_2O_3/SiO_2 and Graphene coated Cr_2O_3/SiO_2 core shell nanoparticles.

Figure 5 shows the optical band gap spectra of the core Cr_2O_3, core shell Cr_2O_3/SiO_2 and Graphene coated Cr_2O_3/SiO_2 core shell nanoparticles. Cr_2O_3 is a p-type semiconductor and its band gap, Eg, can be determined by the following equation:

$$(\alpha hv)^2 = K\,(hv - E_g)$$

Where hv is the photon energy (in eV), α is the absorption coefficient, E_g absorption band gap energy, K is a constant relative to the material. Figure 5 shows the plot of $(\alpha hv)^2$ versus hv. The absorption

band Eg values of core, core shell and Graphene based core shell were 3.04, 2.4 and 1.9 eV. When the particle size decrease there is shifted (blue shift) to a energy with higher amount.

Figure 6 shows the extinction coefficient as a function of photon energy for Cr_2O_3, core shell Cr_2O_3/SiO_2 and Graphene coated Cr_2O_3/SiO_2 core shell nanoparticles. The absorption of materials directly related to the Extinction coefficient can be determined by the relation:

$$k = \frac{\alpha\lambda}{4\pi}$$

where, K is extinction coefficient, α is % absorption coefficient and λ is a wavelength. In Fig. 6, the extinction coefficient of core Cr_2O_3, core shell Cr_2O_3/SiO_2 and Graphene coated Cr_2O_3/SiO_2 core shell nanoparticles. The extinction coefficient becomes exponentially decrease in the coated material SiO_2 and GO, with an increase in photon energy represents that, the loss factor decreases respectively Xiong Liu et al ., 2007.

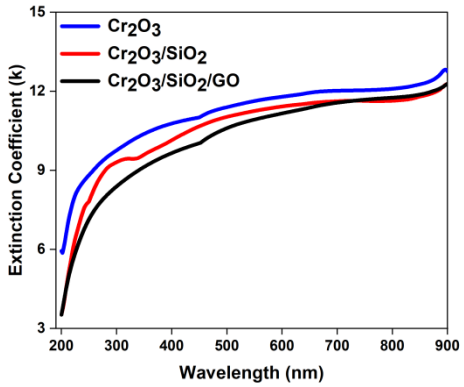

Figure 6 Extinction coefficient of core Cr_2O_3, core shell Cr_2O_3/SiO_2 and Graphene coated Cr_2O_3/SiO_2 core shell nanoparticles.

Figure 7 shows, the plot of refractive index (n) as a function of wavelength (λ) for the core Cr_2O_3, core shell Cr_2O_3/SiO_2 and Graphene coated Cr_2O_3/SiO_2 core shell nanoparticles. The refractive index (n) has been computed using relation

$$n = \frac{1+Ts}{1-Ts}\sqrt{\frac{4Ts}{(1-Ts)^2}-1}$$

where, n is refractive index and T_s is % transmission coefficient. The refractive index values were changed with added the coating materials SiO_2 and GO. It is found to be at a low content, which resulting in higher reflection.

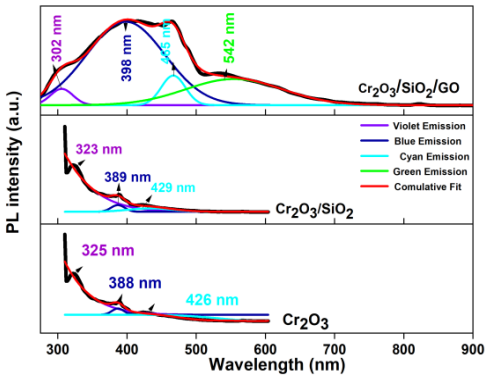

Figure 7 shows, the plot of refractive index (n) as a function of wavelength (λ) for the core Cr_2O_3, core shell Cr_2O_3/SiO_2 and Graphene coated Cr_2O_3/SiO_2 core shell nanoparticles.

The results of optical band gap energy values, Extinction coefficient and refractive index were established, the Graphene coated Cr_2O_3/SiO_2 core shell material has potential application in optoelectronics devices.

3.5 Photoluminescenc Spectrometer

The photoluminescence (PL) spectra for the core Cr_2O_3, core shell Cr_2O_3/SiO_2 and Cr2O3/SiO_2/GO nanoparticles prepared at room temperatures in the range of 300 to 900 nm are shown in Fig. 8. In core Cr_2O_3 sample a broad emission peaks were observed in the range of 325–426 nm, which were attributed to the high purity and perfect crystallinity. The wavelength from 300-400 nm is UV/blue emission, 400 – 500 nm is blue emission and also these peaks were created due to the oxygen vacancy of the Cr_2O_3 core, Cr_2O_3/SiO_2 and Cr_2O_3/SiO_2/GO core shell and 500-600 nm green emission. The emission bands were connected with excitonic reunite of electrons in the conduction band (CB) and hole in the valence band (VB) corresponding to the near band emission transition.

However, the emission peaks were located at ~425 – 455nm, which can be assigned to the transition involving $3d^3$ electrons of the Cr^{3+} ions (Kamari et al., 2019, Zoromba, M. Sh et al., 2019, Almontasser et al., 2020). The emitted wavelength of the oxide material mostly depends on the particles size and morphology. According to this results were come to the end, this core and core shell nanoparticles were well dispersed fine particles, with control crystalline sizes. Besides, the PL result tells that the bio – synthesized core Cr_2O_3, core shell Cr_2O_3/SiO_2 and Cr_2O_3/SiO_2/GO nanoparticles are acceptable material used for optical storage systems.

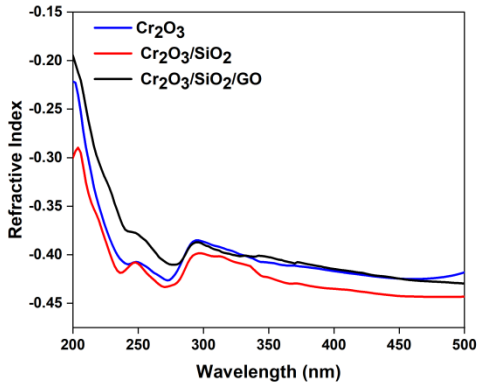

Figure 8. Photoluminescence spectra for the core Cr_2O_3, core shell Cr_2O_3/SiO_2 and Cr_2O_3/SiO_2/GO

3.6 **Cyclic Voltammetry**

The active surface area of the GO based SiO_2 coated Cr_2O_3 electrode were determined from the cyclic voltammetry. The effect of scan rate on the oxidation peak current of GO based SiO_2 coated Cr_2O_3 core shell were studied in the range of 150 mVs^{-1}.The active area found to be 2.1067 cm^2, 2.096 cm^2 and 2.0835 cm^2 for core Cr_2O_3 and core shell Cr_2O_3/SiO_2 and Cr_2O_3/SiO_2/GO. The figure 9 illustrates were the anodic peak current increases with increases with coating material SiO_2 and GO. Fig 9a represents the cyclic voltammetry of core Cr_2O_3, without any faradic activity (without oxidation or reduction) and fig 9b,c depicts CV of core shell

Cr_2O_3/SiO_2 and $Cr_2O_3/SiO_2/GO$ were shows the oxidation peak at 0.21 V and 0.2668 V, reduction peak at 0.32 V and 0.43 V respectively. The redox behavior of the Cr_2O_3 oxidation on the electrode surface were found to be quasi – reversible as can be seen from the peak separation of forward reverse scan of the voltammogram (Fig b and c). The specific capacitances were calculated from the CV curves according to the following equation:

$$C = \frac{Q}{Vm} Fg^{-1}$$

Where C is the specific capacitance (F g^{-1}), m is the mass of the active materials (g), Q is the average charge during the charging and discharging process (C), and V is the potential window (V).

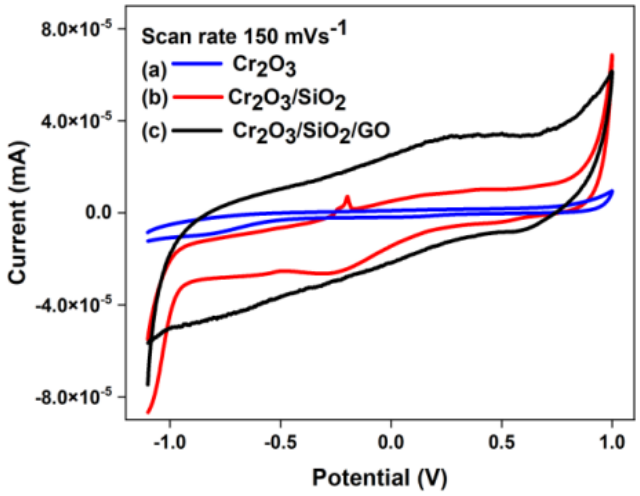

Figure 9 cyclic voltammetry curves of (a) core Cr_2O_3, (b) core shell Cr_2O_3/SiO_2 and (c) Graphene coated Cr_2O_3/SiO_2 core shell nanoparticles.

In this formula the supercapacitor delivered a specific capacitance of 30.23μF/g for core Cr_2O_3 and 151.97μF/g for core shell Cr_2O_3/SiO_2 and 191.28μF/g for $Cr_2O_3/SiO_2/GO$ at a current density of core Cr_2O_3 is 0.664 mA/cm^2, core shell Cr_2O_3/SiO_2 is 0.0338 mA/cm^2 and $Cr_2O_3/SiO_2/GO$ is 0.00449 mA/cm^2.

4. CONCLUSION

The present study shows that Cr_2O_3 core, Cr_2O_3 /SiO_2 core shell and Cr_2O_3/SiO_2 /GO NPs were successfully synthesized by biomethods. The approaches used during the fabrication of $Cr_2O_3/SiO_2/GO$ NPs using the stem extract and studied their morphological and physiochemical properties. The formation of $Cr_2O_3/SiO_2/GO$ NPs have analyzed by the modern techniques of characterization were used. The XRD study shows that the size of Cr_2O_3 core, Cr_2O_3 /SiO_2 core shell and Cr_2O_3/SiO_2 /GO NPs synthesized by biomethod was 58, 40 and 17 respectively. The SEM study shows that Cr_2O_3 core, Cr_2O_3 /SiO_2 core shell and Cr_2O_3/SiO_2 /GO NPs are rods morphology. The EDX shows that synthesized nanoparticles are pure and there is only trace of impurities present in the samples. From the morphography studies the grown Cr_2O_3 core, Cr_2O_3 /SiO_2 core shell and Cr_2O_3/SiO_2 /GO NPs were important for the development of electronic, optical, magnetic and micromechanical devices and the results of all the optical parameters studies of the investigated $Cr_2O_3/SiO_2/GOs$ samples prove that these composites are more suitable in their great potential of optoelectronic devices and UV-shielding coatings.

The results of CV proved that this kind of hybrid supercapacitor has good electrochemical capacitance performance within potential range from -1.2 V to 1.1V for GO based SiO_2 coated Cr_2O_3 core shell. At a current density of core Cr_2O_3 is 0.664 mA/cm^2, core shell Cr_2O_3/SiO_2 is 0.0338 mA/cm^2 and $Cr_2O_3/SiO_2/GO$ is 0.00449 mA/cm^2, the hybrid supercapacitor delivered a specific capacitance of 30.23 μF/g for core Cr_2O_3, 151.97 μF/g for core shell Cr_2O_3/SiO_2 and 191.28 μF/g for $Cr_2O_3/SiO_2/GO$, which is much higher than that of Cr_2O_3 nanoparticles symmetric supercapacitor reported in literatures. In this respect, the $Cr_2O_3/SiO_2/GO$ is a new path is open for the future development of safe and cost-effective electrochemical supercapacitors.

Acknowledgement

We want to thank for SEM analysis centre from Avinash Lingam College, Coimbatore and the UV, PL and CV analysis from V.O.Chidambaram College, Tuticorin involved for this work.

References

1. Choi. S, Bonyani. M, Sun. G.J, Lee. J. K, Hyun. S. K, and Lee. C. 2018. Cr_2O_3 nanoparticle-functionalized WO_3 nanorods for ethanol gas sensors. Applied Surface Science, 432, 241–249.
2. Guo Yu, Zhao Ningning, Zhang Ting, Gong Hujun, Ma Haixia, An Ting, Zhao Fengqi and Hu Rongzu 2019. Compatibility and thermal decomposition mechanism of nitrocellulose/CrO nanoparticles studied using DSC and TG-FTIR. RSC Advances, 9(7): 3927–3937.
3. Rasheed, Rashed Taleb, Easa, Hamssa A and Jassim Liblab S. 2020. AIP Conference Proceedings [AIP Publishing 2nd International Conference on Materials Engineering & Science (IconMEAS 2019) - baghdad, iraq (25â€“29 September 2019)] - Preparation and characterization of Cr_2O_3 nanoparticle prepared by chemical method. AIP Conference Proceedings, 2213, 020202.
4. Ghotekar. S, Pansambal. S, Bilal. M, Pingale. S.S, and Oza. R. 2021. Environmentally friendly synthesis of Cr_2O_3 nanoparticles: Characterization, applications and future perspective ─ a review. Case Studies in Chemical and Environmental Engineering, 3: 100089.
5. Bahrami Kiumars and Karami Zahra. 2018. Core/shell structured ZnO@SiO -TTIP composite nanoparticles as an effective catalyst for the synthesis of 2-substituted benzimidazoles and benzothiazoles. Journal of Experimental Nanoscience, 13(1): 272–283.
6. Haque Fozia. Z, Nandanwar Ruchi, Singh Purnima, Dharavath Kishan, Syed Fazil F. 2016. Effect of Different Acids and Solvents on Optical Properties of SiO_2 Nanoparticles Prepared by the Sol-Gel Process. Silicon.
7. Asmaa M. Abozied, Ayman M, Mostafa. A, Abouelsayed. A.F. Hassan. A.A, Ramadan, Emad. A, Al-Ashkar and Badawi Anis. 2021. Preparation, characterization, and nonlinearoptical properties of graphene oxide thin filmdoped with low chirality metallic SWCNTs. Journal of Materials Research and Technology.
8. Sahu, Sumit Ranjan, Devi, Mayanglambam Manolata, Mukherjee, Puspal, Sen, Pratik, Biswas, Krishanu. 2013. Optical Property Characterization of Novel Graphene-X (X=Ag, Au and Cu) Nanoparticle Hybrids. Journal of Nanomaterials, 2013, 1–9.
9. Al-Awadi. A. S, El-Toni. A. M, Labis. J. P, Khan. A, Ghaithan. H, Al-Zahrani. A. A, Al-Zahrani. S. M. 2021. Mesoporous Organo-Silica Supported Chromium Oxide Catalyst for Oxidative Dehydrogenation of Ethane to Ethylene with CO_2. Catalysts, 11(5), 642.
10. Daniel. T, Balasubramanian V, Joy Jeba Vijila. J, Nishanthi. S.T, Amudhavalli. K, Sivakumar. G, Senthil Siva Subramanian. T and Mohanraj. K. 2021. Photoelectrochemical and photovoltaic cell performances of thermally evaporated Cu_3BiS_3 thin films. Vacuum, Volume, 195: 110707.
11. Makhlouf Salah. A, Bakr Zinab. H, Al-Attar. H and Moustafa. M.S. 2013. Structural, morphological and electrical properties of Cr_2O_3 nanoparticles. Materials Science and Engineering. B, 178(6), 337–343.
12. Xiong Liu, Mark Atwater, Jinhai Wang and Qun Huo. 2007. Extinction coefficient of gold nanoparticles with different sizes and different capping ligands, 58(1), 3–7.
13. Kamari, Halimah Mohamed, Al-Hada, Naif Mohammed, Baqer, Anwar Ali, Shaari, Abdul H and Saion, Elias. 2019. Comprehensive study on morphological, structural and optical properties of Cr_2O_3 nanoparticle and its antibacterial activities. Journal of Materials Science: Materials in Electronics.
14. Zoromba. M. Sh, Bassyouni. M, Abdel-Aziz. M. H, Al-Hossainy. Ahmed F, Salah Numan, Al-Ghamdi. A. A and Eid Mohamed. R. 2019. Structure and photoluminescence characteristics of mixed nickel–chromium oxides nanostructures. Applied Physics A, 125(9), 642.
15. Almontasser Asma, Parveen Azra, Hashim Mohd, Ul-Hamid Anwar and Azam Ameer. 2020. Structural, optical, and antibacterial properties of pure and doped (Ni, Co, and Fe) Cr_2O_3 nanoparticles: a comparative study. Applied Nanoscience.